Title
Dynamical Model and Optimal Turning Gait for Mechanical Rectifier Systems

Journal
IEEE Transactions on Automatic Control, 62(2)

ISSN
0018-9286

Authors
Kohannim, Saba
Iwasaki, Tetsuya

Publication Date
2017

DOI
10.1109/tac.2016.2561700

Peer reviewed

Dynamical Model and Optimal Turning Gait for Mechanical Rectifier Systems

Saba Kohannim and Tetsuya Iwasaki

***Abstract*—Animal locomotion can be viewed as mechanical rectification due to the dynamics that convert periodic body movements to a positive average thrust, resulting in a steady locomotion velocity. This paper considers a general multi-body mechanical rectifier under continuous interactions with the environment, with full rotation and translation in three dimensional space. The equations of motion are developed with respect to body coordinates to allow for direct analysis of maneuvering dynamics. The paper then formulates and solves an optimal turning gait problem for a mechanical rectifier traveling along a curved path, with propulsive forces generated by periodic body deformation (gait). In particular, the gait is optimized to minimize a quadratic cost function, subject to constraints on average locomotion velocity and average angular velocity. The problem is proven to reduce to two separate, tractable minimization problems solvable for globally optimal solutions. The first problem solves for the optimal shape offset that results in turning, while the other solves for the optimal gait that results in locomotion along a straight path. A case study of a locomotor in a fluid environment is presented to demonstrate the utility of the method for robotic locomotor design.**

***Index Terms*—Robotics, optimal control, nonlinear systems, biological systems**

I. Introduction

Robotic vehicle designs have been inspired by locomotion of animals that can efficiently interact with the environment to produce a desired locomotion velocity, and can adapt to environmental changes through modifications in their body movements. Animal locomotion can be regarded as a type of mechanical rectification, in which sustained propulsive forces are produced through the interaction of the environment with the animal's periodic body motions (gaits) [1]–[3]. An essential problem in the design of robotic locomotors inspired from animal locomotion is determining a gait that optimizes an important performance or cost function while satisfying a desired trajectory constraint. This problem has been studied extensively in the literature for various mechanical rectifiers, but due to inherent difficulty, most existing results only provide solutions that are locally optimal.

For locally optimal solutions, a standard approach is based on the nonlinear optimal control theory. In [4], Pontryagin maximum principle is used to characterize the optimal gait of a seven-link biped robot in terms of a two-point boundary value problem, which is solved by heuristic numerical methods. A similar method was used in discrete-time setting [5] to solve for snake-like link structures. Another popular approach is to reduce the problem to a finite dimensional parametric optimization by restricting the variables to the span of selected basis functions (e.g. Fourier series, polynomial, piecewise constant). In [6] and [7], this approach is taken to find optimal gaits for an underwater eel-like robot and for a nonholonomic snakeboard, respectively, by solving a stationarity condition using Newton iteration algorithms. The parametric approach is also used for biped robots with direct numerical optimizations through sequential quadratic programming [8], [9], steepest gradient descent method [10], and a commercial software package [11].

There are a few approaches for computing global solutions of certain optimal gait problems. One approach is inspired by biology, where an optimization problem is formulated over a narrow set of possible gaits that are observed in animal locomotion. In particular, for serpent crawling and eel swimming, the animals exhibit undulatory body movements with waves traveling down the body, which can be parameterized by sinusoidally time-varying curvature with constant amplitudes and linearly decreasing phases over the slender body. Since the parameter space of various gaits is restricted, it is possible to find the globally optimal solution by simulations on gridded parameter points [12] or by analytical perturbation methods [13]. These methods find reasonable gaits, but can miss better gaits that deviate from those observed in biology.

Another approach to globally optimal gaits is to restrict the class of underlying locomotion dynamics rather than the class of possible gaits. Reference [14] considers a general class of mechanical rectifiers that are in continuous interactions with the environment, including swimming, flying, and slithering. A simplified bilinear model is developed under the assumption of small curvature deformation, capturing essential rectifier dynamics necessary for locomotion. An optimal gait problem is then formulated as a minimization of a quadratic cost function over all periodic body movements achievable with a given set of actuators, subject to a constraint on the average locomotion velocity. The globally optimal solution is obtained using generalized eigenvalue computation, and the method's utility is validated by case studies of a link-chain rectifier swimming in water.

The methods mentioned above are primarily used to find optimal gaits for locomotion along a straight line, but the

This material is based upon work supported by the National Science Foundation (NSF) Graduate Research Fellowship under Grant No. DGE-1144087 and an NSF grant no.1068997.

The authors are with the Department of Mechanical and Aerospace Engineering, University of California, Los Angeles, 420 Westwood Plaza, Los Angeles, CA 90095, {sabakohannim,tiwasaki}@ucla.edu.

problem can also be extended for turning motion along a curved path. Turning motion has been studied in the robotics framework by [15]–[18] for biped, quadruped, and hexapod robots. However, in the frameworks of walking on land, optimality is generally defined by the gait with maximum stability to follow a defined path. Planar turning motion has also been investigated by [5], [13], [19] for eel swimming and snake crawling. In all these cases, a constant offset is added to the harmonic shape variable to achieve turning; however, only the harmonic terms are included in the optimization problem and the offsets are set to prescribed values, with no basis for the separation of the offset terms from the periodic terms. Thus, it remains essentially open how to optimize the gait for turning locomotion in three dimensional space while minimizing a general cost function.

In this paper, we address this open problem; we develop a functional model for a general class of mechanical rectifiers in three dimensional space, and extend the approach by [14] to find globally optimal gaits that satisfy a desired steady turning constraint. We consider a multi-body mechanical rectifier with full (six) degrees of freedom (DOF) for position and orientation within the inertial frame, in addition to arbitrary finite degrees of freedom for body shape deformation. The body is assumed to be in continuous contact with its environment, receiving environmental forces that are proportional to the relative velocities with directional preference. This class of rectifier systems has been considered in [14], where the equations of motion are derived within the inertial frame. We build on the previous result and transform the equations of motion into body coordinates in order to provide a comprehensible description of the dynamics for arbitrary three dimensional maneuvers from the "pilot's view", and independent of an inertial frame. Assuming small body deformation, the nonlinear model is reduced to a simplified model that is tractable and captures the essential rectifying dynamics.

An optimal turning gait problem is then formulated for the simplified model as the search for a periodic body movement that minimizes a quadratic cost function while achieving a steady turning motion with prescribed linear and angular velocities on average over each cycle. Similar to the previous methods mentioned above, shape offsets are added to the periodic shape variables to allow for turning motion; however, in this case the shape offsets are not specified *a priori*, but included in the optimization. The problem is shown to reduce equivalently to two separate and simpler minimization problems that are both solvable for globally optimal solutions. The first problem solves for the nominal (fixed) body shape that yields the desired turning rate while minimizing the additional drag due to turning. The second solves for the optimal periodic body movement that would minimize the cost function if the locomotion were achieved at the prescribed tangential speed without the turning constraint, under increased environmental drag and modified body dynamics. Thus, our main result proves a separation principle in optimal turning gait where the cost function and optimization variables can both be decoupled into rotational and translational terms. The rotational problem is a simple convex optimization and we provide an analytical solution, while the translational problem takes the same form as the one solved in [14] in terms of generalized eigenvalues, where a harmonic gait is shown to be optimal. The utility of the developed model and the optimal turning gait results are tested by a numerical case study of an arbitrary swimming locomotor designed to allow thrust generation in roll, pitch, and yaw turning directions.

An abridged conference version of the present paper is in [20] without technical details or proofs. The locomotor case study reported here is new. Some preliminary results on planar turning of an undulating link-chain rectifier have been presented in [21].

Notations: The set of positive integers is denoted by $\mathbb{Z}$. The sets of n by m real and complex matrices are denoted by $\mathbb{R}^{n\times m}$ and $\mathbb{C}^{n\times m}$ respectively. For vectors f and x, the $(i,j)^{th}$ entry of $\partial f/\partial x$ is given by $\partial f_j/\partial x_i$. For a complex matrix X, the transpose, complex conjugate transpose, and real part are denoted by $X^\intercal$, X^*, and $\Re[X]$ respectively. The matrix (or vector) obtained by stacking matrices X_i, $i \in \mathbb{Z}_n$, in a column is denoted by $\mathrm{col}(X_1,\ldots,X_n)$. Similarly, $\mathrm{diag}(X_1,\ldots,X_n)$ denotes the block diagonal matrix with X_i stacked on the diagonal.

II. Mechanical Rectifier System

We consider a general mechanical system composed of multiple rigid bodies that are connected arbitrarily to each other at rigid or flexible joints with rotational and/or linear degrees of freedom. The shape of the system is defined by relative positions and orientations of the multiple bodies, and can be deformed through actuators placed at some of the joints. The multi-body system can rotate and translate in three-dimensional space due to interactive forces resulting from continuous contact with the environment (e.g. water, air, ground). We assume that the gravity effect can be neglected due to e.g. neutral buoyancy of the system in a fluid. When the system interacts with the environment to convert periodic body motion to a net thrust over each cycle, we call it a mechanical rectifier. Such systems would represent animal locomotions or their robotic realizations such as fish and batoid swimming, eel/serpent slithering, and balloon flight with flapping wing.

The environmental force on each body is roughly modeled as a static linear function of the relative velocities seen from the body frame. The linear dependence of the force on velocity is meant to capture the qualitative nature of resistive interactions with the environment in various contexts (hydrodynamic drag in swimming, Coulomb friction in slithering, etc.). The values of the drag coefficients are chosen to quantitatively dictate the net effect over each cycle of body oscillation. For instance, hydrodynamic force in swimming may be modeled by a nonlinear function of the velocity $f(v)$ [22], [23]. However, if the velocity is roughly sinusoidal $v(t) \cong a\sin(\omega t + b)$ during periodic body movements, the net effect of the nonlinear force may

be approximated by a Fourier series truncation to yield the linear term $f(v) \cong \kappa(a)v$ where $\kappa(a)$ is the describing function [24]. The truncated higher order harmonics would have a small impact on the overall behavior if they are damped out due to the low pass filtering effect of the body dynamics with inertia.

The next sections outline the derivation of analytical models for mechanical rectifiers, with supplementary details given in the Appendix. The equations of motion with respect to the inertial frame can be developed through the Euler-Lagrange equation, using a set of generalized coordinates as in [14]. However, our goal is to analyze turning motion of the rectifier with a fixed average locomotion speed and angular velocity. Therefore, we will develop equations of motion with respect to a body frame, so that the dynamics are described independently of the position and orientation with respect to the inertial frame, as a consequence of the symmetry/invariance property of the environmental forces. The equations of motion are then reduced, assuming small body oscillations, to a simpler state space form that is reasonably accurate, tractable, and usable for analytical study of optimal gaits for turning.

A. General equations of motion in the body frame

A mechanical rectifier in three dimensional space has $n = 6 + \ell$ degrees of freedom, where the generalized coordinates $q := \mathrm{col}(w, \psi, \phi) \in \mathbb{R}^n$ are given by the position $w \in \mathbb{R}^3$, orientation $\psi \in \mathbb{R}^3$, and body shape $\phi \in \mathbb{R}^\ell$. The position of the rectifier can be defined as the coordinates w of the center of mass of the entire multi-body system within the inertial frame. The body shape ϕ of the rectifier is given in terms of the kinematic variables specifying the relative position/orientation between bodies within the system (e.g. joint angles). The orientation of the rectifier can be represented by a body frame attached to one of the bodies comprising the rectifier. In particular, ψ can be defined as a set of Euler angles for the body frame with respect to the inertial frame.

The angular velocity of the body frame with respect to the inertial frame, $\varpi \in \mathbb{R}^3$, can be expressed in the body frame as

$$\varpi := P(\psi)\dot{\psi},$$

where $P(\psi) \in \mathbb{R}^{3\times 3}$ is a matrix-valued function uniquely determined from the choice of the Euler angle sequence. The locomotion velocity expressed in the body frame is given by

$$\nu := \mathrm{col}(\nu_x, \nu_y, \nu_z) := \Omega(\psi)\dot{w},$$

where $\Omega(\psi) \in \mathbb{R}^{3\times 3}$ is the orthogonal rotation matrix, and ν_x, ν_y, and ν_z are the velocity components along the respective axes of the body frame. We now define the new velocity variable

$$\rho := \begin{bmatrix} \nu \\ \dot{\xi} \end{bmatrix}, \quad \dot{\xi} := \begin{bmatrix} \varpi \\ \dot{\phi} \end{bmatrix}.$$

The equations of motion for a general mechanical rectifier, with respect to the body frame, can be developed using the Euler-Lagrange equation given by

$$\frac{d}{dt}\left(\frac{\partial \rho}{\partial \dot{q}}\frac{\partial L}{\partial \rho}\right) - \frac{\partial L}{\partial q} = \hbar, \tag{1}$$

where $L := T - V$ is the Lagrangian, $T(q, \rho) \in \mathbb{R}$ is the total kinetic energy of the system, $V(q) \in \mathbb{R}$ is the total potential energy, and $\hbar(t) \in \mathbb{R}^n$ are the generalized forces. Here, ρ is viewed as a function of the generalized coordinates $\rho(q, \dot{q})$, and the equations of motion will be developed in terms of (q, ρ) rather than $(q, \dot{q})$.

The total kinetic energy is the sum of the translational and rotational kinetic energies of all bodies, and can be expressed as

$$T(q, \rho) = \frac{1}{2}m||\nu||^2 + \frac{1}{2}\dot{\xi}^\intercal \mathcal{J}(\phi)\dot{\xi}, \tag{2}$$

where m is the total mass, and $\mathcal{J}(\phi)$ is the moment of inertia matrix. The total potential energy captures the elastic potential energy associated with body deformation and is only a function of the shape of the mechanical rectifier, i.e. $V = V(\phi)$.

The generalized forces consist of environmental forces $\hbar_e(t) \in \mathbb{R}^n$ and actuator input forces $\hbar_a(t) \in \mathbb{R}^n$, so that $\hbar = \hbar_e + \hbar_a$. Let $u(t) \in \mathbb{R}^r$ be the actuator force/torque inputs, and assume that their displacements are linear functions of shape variables given by $\mathsf{B}^\intercal q$ for a coefficient matrix $\mathsf{B} \in \mathbb{R}^{n\times r}$ with its first six rows being zero. Then, the generalized force of actuators can be expressed as $\hbar_a = \mathsf{B}u$. Let us define B to be the bottom $(\ell + 3) \times r$ block of B for later use. The environmental force acting on a small segment on the i^{th} body, at location c within a local frame, with surface area da_i, is modeled as

$$df_i = -\Omega(\psi_i)^\intercal \Delta_i \Omega(\psi_i)\dot{\sigma}_i(\mathsf{c})da_i,$$

where $\Delta_i \in \mathbb{R}^{3\times 3}$ is a constant matrix of drag/friction coefficients, $\dot{\sigma}_i(\mathsf{c}) \in \mathbb{R}^3$ is the velocity of the segment, and $\psi_i \in \mathbb{R}^3$ are the Euler angles of body i. The total virtual work $\delta\mathrm{W}$ is obtained by integrating $(\delta\sigma_i(\mathsf{c}))^\intercal df_i$ over the surface of body i and summing over all the bodies of the rectifier. The generalized environmental forces $\hbar_e$ are then found from $\delta\mathrm{W} = (\delta q)^\intercal \hbar_e$ as

$$\hbar_e = -\begin{bmatrix} \Omega(\psi) & 0 \\ 0 & \Gamma(\psi) \end{bmatrix}^\intercal \begin{bmatrix} \mathcal{C}(\phi) & \mathcal{E}(\phi)^\intercal \\ \mathcal{E}(\phi) & \mathcal{D}(\phi) \end{bmatrix} \begin{bmatrix} \nu \\ \dot{\xi} \end{bmatrix}, \tag{3}$$

for appropriately defined coefficient matrices.

Using the given expressions for kinetic energy, potential energy, and generalized forces, the Euler-Lagrange equation reduces to the following two equations of motion:

$$\begin{aligned} &\mathcal{J}(\phi)\ddot{\xi} + g(\phi, \dot{\xi}) + \mathcal{D}(\phi)\dot{\xi} + \mathcal{E}(\phi)\nu + \mathsf{k}(\phi) = Bu, \\ &m\dot{\nu} + mQ(\varpi)\nu + \mathcal{C}(\phi)\nu + \mathcal{E}(\phi)^\intercal\dot{\xi} = 0, \end{aligned} \tag{4}$$

where the coefficient matrices are defined in the Appendix. The terms $\mathcal{J}(\phi)\ddot{\xi} + g(\phi, \dot{\xi})$ and $m\dot{\nu} + mQ(\varpi)\nu$ are the inertial torques and forces, $\mathcal{D}(\phi)\dot{\xi} + \mathcal{E}(\phi)\nu$ and $\mathcal{C}(\phi)\nu + \mathcal{E}(\phi)^\intercal\dot{\xi}$ capture the environmental torques and forces, $\mathsf{k}(\phi)$ are the torques due to body stiffness, and $u \in \mathbb{R}^r$ are the forces/torques applied through actuators. Because the generalized velocity $\dot{q}$ is replaced by the body-frame variable ρ in (4), all the coefficient matrices are independent of

the rectifier's orientation ψ and position w, due to assumed symmetry of the environmental forces. This property allows us to specify desired nominal locomotion velocity and angular velocity in the optimal gait problem.

B. Approximate model for trimmed locomotion

In order to analyze the locomotion mechanism of a mechanical rectifier (4), and formulate a tractable and meaningful optimal turning gait problem, we develop the simplest approximated model that still captures the essential rectifying dynamics. We focus on a trim condition for steady turning locomotion where the rectifier body moves through space at a constant speed ν and angular velocity ϖ. Since the thrust is generated by rectifying the effect of periodic body oscillation, the actual values of ν and ϖ oscillate around fixed constants. The objective is to develop a simple model that captures the perturbed dynamics around the trim condition, including the thrust generation mechanisms.

In [14], simplified equations of motion for a general mechanical rectifier in a similar form to (4), but in the inertial frame, were developed to capture the dynamics during locomotion *along a straight line*. The simple model was used for analytical study of optimal gaits and was shown to be valid for snake-like undulation and jellyfish-like flapping of link-chain locomotors in comparison with numerical simulations of the original nonlinear model. In their approach, it was assumed that the body oscillated about some nominal posture, defined as a fixed body shape and orientation that allow coasting along a straight line in the absence of any actuator inputs. The oscillation about the nominal posture was assumed small and of order ϵ, and Taylor series expansions were used to reduce the equations to their simplest forms by retaining up to second order $\mathcal{O}(\epsilon^2)$ terms that had essential contribution to the thrust generation.

Here, we use a similar approach to [14], but modify it to make it applicable for turning motion. Since body orientation ψ does not appear in the new equations of motion (4), there is no need to introduce nominal orientation angles. This feature is essential for turning analysis. We consider the nominal body shape ϕ defined as follows. Let $\mathbb{V} \subset \mathbb{R}^3$ be a linear subspace (straight line) indicating the intended direction of locomotion in the body frame. The shape $\phi(t) \equiv \eta \in \mathbb{R}^\ell$ is said to be nominal along $\mathbb{V}$ if

$$\mathsf{k}(\eta) = 0, \quad \mathcal{E}(\eta)\mathbb{V} = 0, \quad \mathcal{C}(\eta)\mathbb{V} \subseteq \mathbb{V}. \tag{5}$$

Under these conditions, $(\varpi, \phi, \dot{\phi}) = (0, \eta, 0)$ satisfies (4) with some $\nu(t) \in \mathbb{V}$ and $u(t) \equiv 0$, which can be physically interpreted as follows. At a nominal shape, the body is at rest with minimum elastic potential ($\mathsf{k}(\eta) = 0$), and the rectifier can coast without changing its orientation or shape under no actuator inputs ($\mathcal{E}(\eta)\mathbb{V} = 0$), while keeping the same direction of locomotion velocity ($\mathcal{C}(\eta)\mathbb{V} \subseteq \mathbb{V}$).

We consider the situation where a small body deformation $\varphi(t) := \phi(t) - \eta$ around a nominal shape η achieves steady turning with nearly constant speed ν and angular velocity ϖ. Without loss of generality, we choose the body frame so that the rectifier travels in the y-axis direction during an intended locomotion; $\mathbb{V} = \{ve_2 : v \in \mathbb{R}\}$, where $v := \nu_y$ is the tangential velocity, and $e_i \in \mathbb{R}^3$ is a vector whose i^{th} entry is one and all others are zero. This setting allows us to neglect higher order terms of angular acceleration $\dot{\varpi}$ and normal velocity components $\delta := \mathrm{col}(\nu_x, \nu_z)$, which are perpendicular to the direction of locomotion. Assuming that φ, δ, and $\dot{\varpi}$ are small and of order ϵ, we use Taylor series expansions, like in [14], and linearize the shape equation or the first equation in (4), as well as the normal velocity equation for $\dot{\delta}$. However, we keep up to the quadratic or $\mathcal{O}(\epsilon^2)$ terms in the tangential velocity equation for $\dot{v}$ to keep the thrust term embedded in $\mathcal{E}(\phi)^\intercal \dot{\xi}$, which would be lost if linearized. Note that neither turning rate ϖ nor locomotion speed v is assumed small, and all the terms associated with these variables are retained.

The general equations of motion in (4) then reduce to (see the Appendix for details)

$$\begin{aligned} \dot{x} &= \mathcal{A}(\varpi, v)x + \mathcal{B}u, \\ \dot{v} &= (\mathsf{b}^\intercal x - \mathsf{a})v + x^\intercal \mathcal{S}(\varpi, v)x, \end{aligned} \qquad x := \mathrm{col}(\varpi, \dot{\varphi}, \delta, \varphi), \tag{6}$$

where $v := \nu_y \in \mathbb{R}$, $\delta := \mathrm{col}(\nu_x, \nu_z) \in \mathbb{R}^2$, and $\varphi := \phi - \eta \in \mathbb{R}^\ell$. All the coefficients are a function of the nominal shape η. Coefficients a, b, and $\mathcal{B}$ are constant scalar, vector, and matrix, and $\mathcal{A}(\varpi, v)$ and $\mathcal{S}(\varpi, v)$ are affine in $\mathrm{col}(\varpi, v)$ except that the last ℓ columns of $\mathcal{A}(\varpi, v)$ have additional terms that are quadratic in ϖ. Furthermore, $\mathcal{S}(\varpi, v)$ is symmetric and has zeros in its first 3×3 block. The parameter a is positive, representing the drag from the environment under the nominal condition $x = 0$. These properties become useful when formulating and solving the optimal turning gait problem.

The definition of nominal shape in (5) may not be the best for turning motion analysis since the trim condition results in coasting along a straight line. Alternatively, a nominal shape could be defined to maintain a specified locomotion speed and nonzero angular velocity given a known constant actuator input to keep the shape and a fictitious thrust to sustain the speed. However, finding such a nominal shape is strenuous as it requires solving a complex nonlinear vector equality. Instead, we define the nominal shape by more tractable condition (5) that is generically satisfied by well-designed mechanical rectifiers with streamlined bodies, like those found in nature.

The nominal shape would typically have some symmetry to maintain straight coasting, but body oscillation around an asymmetric shape can be needed for turning. We use model (6) and optimal gait analysis to find the optimal body shape offset that satisfies the desired angular velocity. This process is guaranteed to work only when the desired turning can be achieved by small body shape offsets because model (6) assumes small body deformation around a nominal shape. However, a large body shape offset that achieves higher desired turning rates may be found through an iteration process, where the optimal gait analysis defines the nominal shape used in the next

iteration step, which maintains a specific angular velocity at a desired locomotion speed.

III. Optimal turning locomotion

We will formulate an optimal turning gait problem and provide a solution to find the best body oscillation of the mechanical rectifier that achieves steady locomotion with a desired speed and turning rate on average. The problem formulation and solution are based on the simplified model in (6); however, functionality of the result will be confirmed later for the original model (4) through a case study.

A. Problem statement

We seek the optimal periodic gait $\varphi(t)$ and corresponding periodic control input $u(t)$ that minimizes a quadratic cost function, subject to constraints on the average locomotion velocity v and angular velocity ϖ, with normal velocities δ oscillating about zero. The optimal turning gait problem is formulated for the mechanical rectifier (6) as follows:

$$\min_{\tau\in\mathbb{R}} \ \min_{u\in\mathbb{P}_\tau} \quad \frac{1}{\tau}\int_0^\tau z^\intercal \Upsilon z dt, \quad z := F(s)\begin{bmatrix} x \\ u \end{bmatrix}, \tag{7}$$

$$\text{subject to} \quad \frac{1}{\tau}\int_0^\tau v\,dt = v_o, \tag{8}$$

$$\frac{1}{\tau}\int_0^\tau y\,dt = y_o, \quad y := \mathcal{C}x, \tag{9}$$

where we assume that system (6) admits a τ-periodic solution (x, v) in response to τ-periodic input u. The optimal periodic control input $u \in \mathbb{P}_\tau$ and its period $\tau > 0$ are to be found, where $\mathbb{P}_\tau$ is the set of possibly vector-valued τ-periodic signals. The objective function is the average value of a quadratic form $z^\intercal \Upsilon z$, where Υ is a constant symmetric matrix, and $z \in \mathbb{P}_\tau$ is a selected performance output specified by filtering $\varsigma := \mathrm{col}(x, u) \in \mathbb{P}_\tau$ through a transfer function $F(s)$.[1] The constraints are imposed on the average values of v and y with desired values v_o and y_o. Here, we let $y := \mathrm{col}(\varpi, \delta)$ be the constrained output with target value $y_o := \mathrm{col}(\varpi_o, \delta_o)$, and choose $\mathcal{C}$ accordingly. A typical value of target normal velocity is zero ($\delta_o = 0$), although we allow nonzero values.

The objective function in (7), which is quadratic in variable $\varsigma := \mathrm{col}(x, u)$, is defined in terms of $F(s)$ and Υ. For technical simplicity, we assume that these filter and weight are chosen such that the bias term $\bar{\varsigma} := \frac{1}{\tau}\int_0^\tau \varsigma\,dt$ has no contribution to the value of the objective function. It can readily be verified that the assumption is satisfied if and only if $\bar{\varsigma}^\intercal \Pi(0)\bar{\varsigma} = 0$ holds for the frequency weight $\Pi(j\omega) := F(j\omega)^* \Upsilon F(j\omega)$. Even with this assumption, (7) captures useful cost functions through appropriate choices of $F(s)$ and Υ. Table I gives examples of such objective integrands that are practically important, together with the corresponding frequency weights $\Pi(j\omega)$, where U and W are defined such that $\dot{\zeta} := \mathrm{col}(\varpi, \dot{\varphi}) = U^\intercal x$ and $\dot{\varphi} = W^\intercal x$. The input power and shape derivative have nonzero $\Pi(0)$, but it can be verified that $\bar{\varsigma}^\intercal \Pi(0)\bar{\varsigma}$ is zero by noting that the bias of $\dot{\varphi}$ is zero. Other costs can also be defined with possibly discontinuous function $\Pi(j\omega)$. For instance, if velocity ripples are undesired, the oscillation amplitudes of ϖ and δ can be penalized by choosing $\Pi(j\omega) = \mathrm{diag}(\mathcal{C}^\intercal\mathcal{C}, 0)$ for $\omega \neq 0$ and $\Pi(0) = 0$. Finally, a cost can be given as a linear combination of various costs.

[1] $z = F(s)\varsigma$ under an appropriately chosen initial condition that makes the output τ-periodic without transient.

TABLE I: Objective Functions

Quantity	Objective Function	$\Pi(j\omega)$
Input Power	$\frac{1}{\tau}\int_0^\tau \dot{\zeta}^\intercal B u\,dt$	$\frac{1}{2}\begin{bmatrix} 0 & UB \\ B^\intercal U^\intercal & 0 \end{bmatrix}$
Input Torque Rate	$\frac{1}{\tau}\int_0^\tau \|\|\dot{u}\|\|^2 dt$	$\begin{bmatrix} 0 & 0 \\ 0 & \omega^2 I \end{bmatrix}$
Shape Derivative	$\frac{1}{\tau}\int_0^\tau \|\|\dot{\varphi}\|\|^2 dt$	$\begin{bmatrix} WW^\intercal & 0 \\ 0 & 0 \end{bmatrix}$

B. Problem reformulation using phasors

Solving the optimal gait problem in (7)-(9) for a globally optimal solution is difficult. For tractability, we reformulate the problem assuming small body deformation φ and truncating its higher order terms.

Let us start by introducing some notation and providing a brief review of mathematical preliminaries. A periodic signal $u \in \mathbb{P}_\tau$ can be approximated by its Fourier series

$$u(t) = \bar{u} + \sum_{k=1}^{h} \Re[\hat{u}_k e^{j\omega k t}], \tag{10}$$

where $h \in \mathbb{Z}$ can be arbitrarily large, $\omega := 2\pi/\tau$ is the fundamental frequency, $\bar{u} \in \mathbb{R}^r$ is the bias, and $\hat{u}_k \in \mathbb{C}^r$ is the phasor for the k^{th} harmonic term. We denote the phasor of u as $\hat{u} := \mathrm{col}(\hat{u}_1, \ldots, \hat{u}_h)$. For a transfer function $F(s)$, we define

$$F_\omega^h := \mathrm{diag}(F(j\omega), F(j2\omega), \ldots, F(jh\omega)). \tag{11}$$

The notations $\bar{u}$, $\hat{u}$, and F_ω^h will be used for generic periodic signals and transfer functions. The following result is elementary and can be proven by straightforward calculations (hence a proof is omitted).

Lemma 1: Let periodic signals $z, \varsigma \in \mathbb{P}_\tau$ and a transfer function $F(s)$ be given. Then

$$z = F(s)\varsigma \quad \Rightarrow \quad \bar{z} = F(0)\bar{\varsigma}, \quad \hat{z} = F_\omega^h \hat{\varsigma}.$$

For signals $x, y \in \mathbb{P}_\tau$ of the form (10), we have

$$\frac{1}{\tau}\int_0^\tau x(t)^\intercal y(t)\,dt = \bar{x}^\intercal \bar{y} + \frac{1}{2}\sum_{k=1}^{h} \Re[\hat{x}_k^* \hat{y}_k].$$

We now reformulate the optimal gait problem. One factor that makes the problem difficult is the ripples in the locomotion velocity; if $v(t)$ were constant, the analysis would be easier. We realize this ideal situation by adding a fictitious force $\varepsilon(t)$, with zero average, to the right hand side of the $\dot{v}$ equation in (6). Consider the situation where τ-periodic inputs $u, \varepsilon \in \mathbb{P}_\tau$ for (6), with $\varepsilon(t)$ specifically

chosen to regulate the swim speed $v(t)$, result in constant locomotion velocity $v(t) \equiv v_o$ and τ-periodic response $x(t)$. Approximate $u, x \in \mathbb{P}_\tau$ by truncations of the Fourier series as in (10) for a chosen $h \in \mathbb{Z}$. Assume that the bias term $\bar{\varphi}$ and all the harmonic terms $\hat{x}$ are small and of order ϵ, and neglect the $\mathcal{O}(\epsilon^2)$ and $\mathcal{O}(\epsilon^3)$ terms, respectively, in the $\dot{x}$ and $\dot{v}$ equations in (6). We equate the periodic terms in the first equation of (6) to obtain

$$\hat{x}_k = M(jk\omega)\hat{u}_k, \quad M(s) := \big(sI - \tilde{\mathcal{A}}(\varpi_o, v_o)\big)^{-1}\mathcal{B},$$

where $\tilde{\mathcal{A}}$ is defined to be identical to $\mathcal{A}$ except that the linear terms of ϖ in the first three columns are multiplied by two. The bias terms in the first equation of (6) give

$$\bar{x} = H\bar{u}, \quad H := -\mathcal{A}(\varpi_o, v_o)^{-1}\mathcal{B}.$$

Using the above expression, the angular and normal velocity constraint in (9) can be rewritten as

$$\mathcal{H}\bar{u} = y_o, \quad \mathcal{H} := \mathcal{C}H, \tag{12}$$

Since we assumed a fictitious force ε, with zero average, is applied to keep $v \equiv v_o$, the average of the velocity equation in (6) over one cycle should also be zero. Averaging (6), we replace the velocity constraint integral in (8) by

$$\frac{1}{\tau}\int_0^\tau \Big((\mathfrak{b}^\mathsf{T}x - \mathfrak{a})v_o + x^\mathsf{T}\mathcal{S}(\varpi, v_o)x\Big)dt = 0, \tag{13}$$

yielding the thrust-drag balance at $v(t) \equiv v_o$ with no fictitious forcing on average. The integral in (13) can be converted to a quadratic constraint in $\bar{u}$ and $\hat{u}$ using Lemma 1 as follows:

$$\hat{u}^* Y_\omega^h \hat{u} - \breve{u}^\mathsf{T} Z \breve{u} = 1,$$

where $\breve{u} := \mathrm{col}(\bar{u}, 1)$ and

$$\begin{aligned} &Y(j\omega) := M(j\omega)^*\mathcal{S}(\varpi_o, v_o)M(j\omega)/(2\mathfrak{a}v_o), \\ &Z := -\begin{bmatrix} \nabla & \mathfrak{d} \\ \mathfrak{d}^\mathsf{T} & 0 \end{bmatrix}, \qquad \begin{aligned} &\mathfrak{d} := H^\mathsf{T}\mathfrak{b}/(2\mathfrak{a}), \\ &\nabla := H^\mathsf{T}\mathcal{S}(\varpi_o, v_o)H/(\mathfrak{a}v_o). \end{aligned} \end{aligned} \tag{14}$$

Similarly, the objective integral in (7) can equivalently be written by $\hat{u}^* X_\omega^h \hat{u}$, where

$$X(j\omega) := \frac{1}{2}\begin{bmatrix} M(j\omega) \\ I \end{bmatrix}^* \Pi(j\omega) \begin{bmatrix} M(j\omega) \\ I \end{bmatrix}. \tag{15}$$

In summary, the original optimal gait problem formulated in (7)-(9) is approximated by the following quadratic optimization problem:

$$\min_{\omega \in \mathbb{R}} \min_{\substack{\hat{u} \in \mathbb{C}^{rh} \\ \bar{u} \in \mathbb{R}^r}} \hat{u}^* X_\omega^h \hat{u} \quad \text{s.t.} \quad \begin{aligned} &\hat{u}^* Y_\omega^h \hat{u} = 1 + \breve{u}^\mathsf{T} Z \breve{u}, \\ &\mathcal{H}\bar{u} = y_o, \end{aligned} \tag{16}$$

which is to be solved for the control bias $\breve{u} := \mathrm{col}(\bar{u}, 1)$ and the control phasor $\hat{u}$.

Since the cost or performance function is generally chosen to represent a physical quantity such as energy cost or a vector norm, it is a valid assumption for the cost to be positive. Due to the environmental drag $\mathfrak{a} > 0$, coasting without deceleration is impossible, and there will always be a nonzero cost for any locomotion at nonzero (linear or angular) velocity. Thus we impose the following.

Assumption 1: Consider the optimization problem in (16). The constraints are feasible, and the value of the objective function is positive on the feasible set for any nonzero v_o or ϖ_o and for any $\mathfrak{a} > 0$.

The assumed property turns out to have favorable implications to tractability of the optimization problem as shown in the next section.

C. Optimal turning gait

The optimal gait problem for locomotion along a straight line is a special case of (16), and has been solved in [14]. However, the additional turning rate constraint makes it more difficult. For straight locomotion without turning ($y_o = 0$), zero bias $\bar{u} = 0$ satisfies the second constraint in (16) making $\breve{u}^\mathsf{T} Z \breve{u} = 0$, and problem (16) reduces to

$$\min_{\omega \in \mathbb{R}} \min_{\hat{u} \in \mathbb{C}^{rh}} \hat{u}^* X_\omega^h \hat{u} \quad \text{s.t.} \quad \hat{u}^* Y_\omega^h \hat{u} = 1. \tag{17}$$

While this problem is nonconvex since matrices X_ω^h and Y_ω^h are generally indefinite, [14] has shown that the problem can be equivalently converted to a generalized eigenvalue computation using the S-procedure [25]. For the turning locomotion, however, there are two equality constraints on mixed real ($\bar{u}$) and complex ($\hat{u}$) variables, and direct application of the S-procedure is conservative (inaccurate). One could eliminate the linear equality constraint[2] by solving it for $\bar{u}$, but we take a different approach to gain insights into the turning problem.

Our approach is to reduce the problem to two tractable problems by proving a separation principle under the property in Assumption 1. First note that the cost $\hat{u}^* X_\omega^h \hat{u}$ is small if the oscillation amplitude $\|\hat{u}\|$ is small. The thrust-drag balance, i.e. the first constraint in (16), indicates that $\|\hat{u}\|$ is smaller if $\breve{u}^\mathsf{T} Z \breve{u}$ is smaller. Hence, the term $\breve{u}^\mathsf{T} Z \breve{u}$ can be thought of as the cost associated with turning. Indeed, this term is nonnegative as shown below.

Lemma 2: Suppose Assumption 1 holds. Then

$$\breve{u} = \mathrm{col}(\bar{u}, 1), \quad \mathcal{H}\bar{u} = y_o \quad \Rightarrow \quad \breve{u}^\mathsf{T} Z \breve{u} \geq 0. \tag{18}$$

Proof: Suppose condition (18) does not hold. Then there is a $\bar{u}$ such that $\mathcal{H}\bar{u} = y_o$ but $\breve{u}^\mathsf{T} Z \breve{u} < 0$. Since Z is proportional to $1/\mathfrak{a}$, an appropriate scaling of $\mathfrak{a}$ can make $1 + \breve{u}^\mathsf{T} Z \breve{u} = 0$. For this value of $\mathfrak{a}$, $\hat{u} = 0$ is a feasible control input that satisfies constraint (16), and makes the cost $\hat{u}^* X_\omega^h \hat{u} = 0$. Since this contradicts the original assumption, condition (18) must hold. ∎

Thus, the minimum value of $\breve{u}^\mathsf{T} Z \breve{u}$ is zero and is achieved when the input bias $\bar{u}$ is set to zero for straight locomotion ($y_o = 0$) as in [14]. For general turning locomotion ($y_o \neq 0$), we may minimize the turning cost $\breve{u}^\mathsf{T} Z \breve{u}$ separately by choosing $\bar{u}$. This idea is formally justified as follows.

Lemma 3: Consider problem (16) and

$$\min_{\omega \in \mathbb{R}} \min_{\hat{u} \in \mathbb{C}^{rh}} \hat{u}^* X_\omega^h \hat{u} \quad \textit{s.t.} \quad \hat{u}^* R_\omega^h \hat{u} = 1, \tag{19a}$$

$$\mu := \min_{\bar{u} \in \mathbb{R}^r} \breve{u}^\mathsf{T} Z \breve{u} \quad \textit{s.t.} \quad \mathcal{H}\bar{u} = y_o, \tag{19b}$$

[2]We thank Prof. Lieven Vandenberghe for pointing this out.

where

$$R(j\omega) := Y(j\omega)/(1+\mu), \quad \breve{u} := \mathrm{col}(\bar{u}, 1).$$

Suppose Assumption 1 holds. Then, problem (19) and problem (16) are equivalent in the sense that they have the equal value of the optimal cost function and the same optimizer solution.

Proof: It suffices to show that problems (16) and (19), excluding the minimization over ω, are equivalent for each fixed ω. Let γ_1 be the optimal value of the cost function in (16) with optimizer $(\bar{u}_1, \hat{u}_1)$, let γ_2 be the optimal value of the cost in (19a) with optimizer $\hat{u}_2$, and let $\bar{u}_2$ be an optimizer for (19b). Define

$$\begin{aligned} \alpha_i &:= 1 + \breve{u}_i^{\mathsf{T}} Z \breve{u}_i, & \breve{u}_i &:= \mathrm{col}(\bar{u}_i, 1), \\ \mathtt{R}_i &:= Y_\omega^h / \alpha_i, & \hat{u}_o &:= \sqrt{(\alpha_2/\alpha_1)}\hat{u}_1, \end{aligned}$$

for $i = 1, 2$. Because (18) holds, α_i is always positive, and by definition, $\mathtt{R}_2 = R_\omega^h$. We will show that problems (16) and (19) are equivalent by showing $\gamma_1 \le \gamma_2$ and $\gamma_2 \le \gamma_1$.

The proof for $\gamma_1 \le \gamma_2$ is simple. Because $\hat{u}_2^* Y_\omega^h \hat{u}_2 = 1 + \mu$ where $\mu = \breve{u}_2^{\mathsf{T}} Z \breve{u}_2$, the parameter $(\bar{u}_2, \hat{u}_2)$ satisfies both constraints in problem (16) and is a possible solution to (16). However, since γ_1 is the optimal solution to (16), it follows that $\gamma_1 \le \hat{u}_2^* X_\omega^h \hat{u}_2 = \gamma_2$. To show the other direction, note that the optimizer $(\bar{u}_1, \hat{u}_1)$ satisfies the constraints in (16), and hence $\hat{u}_1^* \mathtt{R}_1 \hat{u}_1 = 1$. We then see that $\hat{u}_o^* \mathtt{R}_2 \hat{u}_o = \hat{u}_1^* \mathtt{R}_1 \hat{u}_1 = 1$, so that $\hat{u}_o$ satisfies the constraint in (19a). It now follows that

$$\gamma_2 \le \hat{u}_o^* X_\omega^h \hat{u}_o = (\alpha_2/\alpha_1)\hat{u}_1^* X_\omega^h \hat{u}_1 \le \gamma_1,$$

where the first inequality holds because γ_2 is the optimal solution to (19a), and the second inequality holds since $\bar{u}_2$ is the optimal solution to (19b) and therefore $\alpha_2 \le \alpha_1$. This completes the proof. ∎

Lemma 3 proves that the optimization problem in (16) can be reduced, equivalently, to two minimization problems, where the optimal bias term is found *separately* from the optimal periodic component. The physical interpretation of (19b) is the minimization of the environmental drag due to the bias $\bar{u}$, given by $\breve{u}^{\mathsf{T}} Z \breve{u}$, with the achievement of the desired turning rate ϖ_o. Equivalently, it can be seen as finding the optimal nominal body shape of the rectifier to reduce the environmental drag effect. According to Lemma 3, the optimal bias offset is independent of the effects of the periodic component or even the choice of cost functions. On the other hand, (19a) has the same form as (17), and is essentially the optimal straight locomotion problem with the modification of the velocity constraint, which compensates for the drag effect μ due to the turning component.

The phasor optimization problem in (19a) can be solved using a previous result for straight locomotion (Lemmas 2 and 3 in [14]). The result shows that the optimal value of the cost $\hat{u}^* X_\omega^h \hat{u}$ is independent of h, meaning that the optimum can always be achieved by a purely sinusoidal input and no further reduction of the cost is possible by a general periodic input. The optimal cost can be found from the generalized eigenvalues of the pair $(X(j\omega), R(j\omega))$ with a line search over ω, and the phasor of the optimal input is given as the corresponding eigenvector.

For the bias optimization problem in (19b), $\breve{u}^{\mathsf{T}} Z \breve{u}$ is an indefinite quadratic form, and hence is not convex. However, it turns out that the objective function is convex on the feasible set under Assumption 1. Therefore, the problem has only one local minimum, and the global minimizer can be found by a local algorithm or convex programming. In fact, the problem admits a closed form solution of the global minimizer as follows.

Lemma 4: Consider the problem (19b). Suppose the problem is feasible and condition (18) holds. Then an optimizer is given by

$$\bar{u}_\flat = \bar{u}_o - N(N^{\mathsf{T}} \nabla N)^\dagger N^{\mathsf{T}} (\nabla \bar{u}_o + \mathtt{d}), \tag{20}$$

where $(\cdot)^\dagger$ denotes the Moore-Penrose inverse, and

$$N := I - \mathcal{H}^\dagger \mathcal{H}, \quad \bar{u}_o = \mathcal{H}^\dagger y_o.$$

Proof: The result follows from a standard linear algebra result [26]. ∎

We can now summarize the main result. Consider the optimal turning gait problem given by (7)-(9) for the mechanical rectifier in (6) with desired locomotion speed v_o, turning rate ϖ_o, and cost weights Υ and $F(s)$. Suppose the objective function value is zero when u and x are constant solutions of (6). Then, based on the reformulation procedure in Section III-B, the problem reduces, approximately, to the quadratic optimization given by (16), where matrices $X(\omega)$, $Y(\omega)$, Z, and $\mathcal{H}$ are defined in (14), (15), and (12). The optimizers of the two problems are related by (10). The globally optimal solution to (16) is given by the following result.

Theorem 1: Consider the optimal turning gait problem given by (16). Suppose Assumption 1 holds. Then the optimal bias $\bar{u}_\flat$ is given by (20), and optimal phasor $\hat{u}_\flat$ and frequency $\omega_\flat$ can be found as follows. For each $\omega > 0$, define

$$R(\omega) := Y(\omega)/(1 + \breve{u}_\flat^{\mathsf{T}} Z \breve{u}_\flat), \quad \breve{u}_\flat := \mathrm{col}(\bar{u}_\flat, 1),$$

and let λ_ω be the largest real generalized eigenvalue of the pair $(X(\omega), R(\omega))$ that satisfies the condition $X(\omega) \ge \lambda_\omega R(\omega)$. Let $\hat{u}_\omega$ be the eigenvector corresponding to λ_ω, normalized such that $\hat{u}_\omega^* R(\omega) \hat{u}_\omega = 1$. The optimal frequency $\omega_\flat$ is given by ω that minimizes λ_ω, and the optimal phasor $\hat{u}_\flat$ is the corresponding eigenvector $\hat{u}_{\omega_\flat}$.

Proof: Problem (16) can be equivalently split into the bias and harmonics (phasor) optimizations in (19) as shown in Lemma 3. The optimal bias $\bar{u}_\flat$ is given by Lemma 4, and the optimal phasor $\hat{u}_\flat$ is obtained from the result in [14] as described. ∎

Theorem 1 states that the optimal control input for the original problem (7)–(9) can be approximately given by the exact solution $u_\flat(t)$ to the reformulated problem (16). The optimal solution $u_\flat(t)$ is purely sinusoidal and has the form

$$u_\flat(t) = \bar{u}_\flat + \Re[\hat{u}_\flat e^{j\omega_\flat t}],$$

where $\bar{u}_\flat$ and $\hat{u}_\flat$ are found by an explicit formula and eigenvalue computation. The optimal frequency $\omega_\flat$ can be found through a line search by gridding the frequency axis and plotting the optimal cost value λ_ω as a function of ω. The optimal gait, or body shape $\varphi_\flat(t)$ corresponding to $u_\flat(t)$, is also sinusoidal and its bias $\bar{\varphi}_\flat$ and phasor $\hat{\varphi}_\flat$ are found by computing $(\bar{x}_\flat, \hat{x}_\flat)$ using the equations following (10). Note that the optimal bias shape $\bar{\varphi}_\flat$ is independent of the cost function.

IV. Numerical example: The H-swimmer

This section demonstrates the utility of the optimal turning gait problem formulation and solution through numerical examples of an arbitrary locomotor swimming in water. The mechanical rectifier is H-shaped, and is composed of a main body (54.5×9.1 mm, 0.33 g) with six degrees of freedom of translation and rotation, and twenty identical panels (9.1×9.1 mm, 0.083 g each) connected at rotational joints, each with one degree of freedom for a total of $n = 26$ degrees of freedom (Fig. 1). Half of the panels are located in front of the main body, divided between right and left sides (arms), and can rotate along the pitch direction, and half of the panels are located behind the main body, divided between right and left sides (legs), and can rotate along the yaw direction. The rectifier's total length along the y-axis is 100 mm, and its width along the x-axis is 54.5 mm. It is placed in a fluid environment, subject to hydrodynamic forces and torques that interact with the body motion to produce thrust for locomotion. The hydrodynamic forces acting on each panel are approximated by linear functions of the relative velocities of the respective segments; $f_{n_i} = c_{n_i} v_{n_i}$ and $f_{t_i} = c_{t_i} v_{t_i}$ in the normal and tangential directions, where $(c_{n_i}, c_{t_i}) = (41, 0.62)$ mN·s/m for the small panels and $(c_n, c_t) = (60, 0.88)$ mN·s/m for the main body. All the model parameter values are set for physical plausibility from experimental data of leech swimming [23].

The body frame is attached to the main body as shown in Fig. 1, and its Euler angles $\psi \in \mathbb{R}^3$ and angular velocity $\varpi \in \mathbb{R}^3$ represent the orientation and turning rate of the rectifier. The joint angles $\phi \in \mathbb{R}^{20}$ specify the body shape, and are defined so that $\phi = 0$ when the arms and legs are stretched along the y-axis. Each joint is actuated by a torque input, such that $u(t) \in \mathbb{R}^{20}$, and the adjoining panels are connected by linear bending stiffnesses 3×10^{-4} Nm/rad. Finally, the nominal shape is set to be straight ($\eta = 0$), where the flexible joints are at rest.

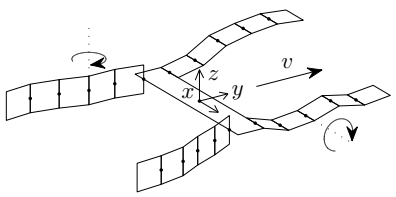

Fig. 1: Swimming locomotor model consisting of $\kappa = 21$ bodies and $n = 26$ degrees of freedom

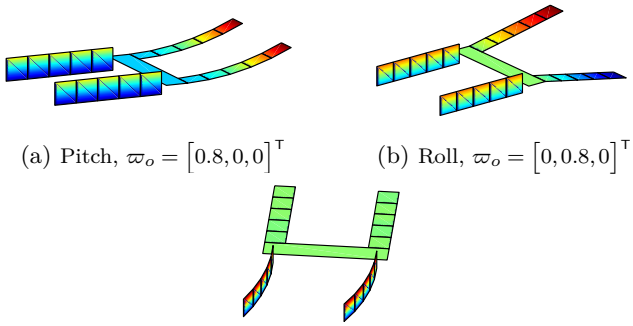

(a) Pitch, $\varpi_o = \begin{bmatrix} 0.8, 0, 0 \end{bmatrix}^\mathsf{T}$ (b) Roll, $\varpi_o = \begin{bmatrix} 0, 0.8, 0 \end{bmatrix}^\mathsf{T}$

(c) Yaw, $\varpi_o = \begin{bmatrix} 0, 0, 0.8 \end{bmatrix}^\mathsf{T}$

Fig. 2: Optimal shape with only bias of the joint angles $\bar{\varphi}_\flat$, around which the body oscillates

This particular locomotor design serves two features. The first is that it is not replicating any particular underwater animal that could give us a reasonable gait without using optimal gait analysis. The second feature is that it allows for torque production in any direction of rotation such that a bias shape $\bar{\varphi}$ exists for any feasible value of the desired angular velocity ϖ_o. This can be better understood by Fig. 2, which shows the optimal bias shapes for basic pitch, roll, and yaw rotations calculated from (20). Pure pitch rotation is achieved by a body shape with left-right symmetry where the arms are curled up along the radius of rotation. Similarly, pure yaw rotation is achieved by the legs curving along the radius of rotation about the z-axis. Pure roll rotation, however, requires asymmetry in the body where one arm pushes the fluid upward and the other arm pushes the fluid downward.

We find the optimal torque input, optimal frequency, and optimal body shape for the three cost functions provided in Table I subject to an average locomotion velocity of $v_o = 100$ mm/s, an average angular velocity of $\varpi_o = \text{col}(75, 75, 400)$ rad/ks, and average $\delta_o = \text{col}(0, 0)$ mm/s. Table II gives the optimal frequencies and the average values of the steady state velocities obtained by simulating the simplified model (6). The optimal frequencies for the three cost functions range between 2 Hz to 4 Hz. The results show that average velocities close to the desired values are achieved for shape-derivative and torque-rate optimizations; however, there are some large errors in the simulated velocities for power optimization. These errors are due to the large harmonics of the angular velocity $\hat{\varpi}$ that violate the assumption that $\hat{\varpi}$ is of order ϵ. The errors can be reduced, if desired, by penalizing a linear combination of power and angular velocity oscillations.

Minimization of each cost function leads to a distinct gait whose optimality is not obvious from physical intuition. Snapshots of these optimal gaits over one period are shown in Figs. 3-5. Thrust generation in the power optimal gait is achieved by the arms sending asymmetrical waves down the right and left sides of the body, while the legs oscillate from side to side with small amplitudes (Fig. 3). The oscillation amplitudes are larger on the left hand side to achieve the desired turning. This asymmetrical gait has a lower power cost than a gait with symmetrical waves

TABLE II: Target values, optimal frequencies, and simulated velocities of the simplified model (6)

objective	ω_b [Hz]	v [mm/s]	δ [mm/s]	ϖ [rad/ks]
(Target Value)	—	100	$\begin{bmatrix}0\\0\end{bmatrix}$	$\begin{bmatrix}75\\75\\400\end{bmatrix}$
Power	2.00	101.0	$\begin{bmatrix}-1.7\\-0.1\end{bmatrix}$	$\begin{bmatrix}100\\85\\499\end{bmatrix}$
Shape	2.26	99.5	$\begin{bmatrix}-0.2\\0.0\end{bmatrix}$	$\begin{bmatrix}75\\75\\413\end{bmatrix}$
Torque	3.66	98.8	$\begin{bmatrix}-1.8\\0.0\end{bmatrix}$	$\begin{bmatrix}73\\69\\394\end{bmatrix}$

traveling down the right and left sides of the locomotor. The shape-derivative cost is minimized when the legs use a flapping motion to propel the locomotor forward, similar to the gait in jellyfish swimming (Fig. 4). This gait is desirable because it minimizes large changes in the body shape and allows the main body to remain steady without large oscillations about its orientation. However, it comes at a price of very large torque and power costs. In the optimal torque-rate gait, the legs synchronously oscillate from side to side at a relatively high frequency, similar to the motion of caudal fins in fish (Fig. 5). This gait saves input torque magnitude, but sacrifices large body shape changes and yawing motion.

Figures 3-5 show that it is optimal to use either arms or legs to generate thrust for locomotion, but it is not desirable to combine all four limb movements. This is a counterintuitive result (valid at least for the simplified model) that one would not be able to predict without using the optimal gait theory. Furthermore, the left-right asymmetry in the optimal gaits resulting from turning requirement, which is most prevalent in power optimization, demonstrates the following point. Although the harmonic term of the body shape is found by solving a problem of the same form as the straight locomotion problem, the oscillatory component of the optimal gait is still a function of the desired angular velocity due to the dependence of $X(\omega)$ and $Y(\omega)$ on ϖ_o.

In order to analyze the accuracy of the optimal gait result from the simplified model (6), we look at the simulated velocities of the original nonlinear model (4) given in Table III. The different gaits result in different accuracies depending on how well they satisfy the assumptions on small

TABLE III: Simulated velocities of the original model (4)

objective	v [mm/s]	δ [mm/s]	ϖ [rad/ks]
Power	87.2	$\begin{bmatrix}0.2\\1.9\end{bmatrix}$	$\begin{bmatrix}84\\60\\312\end{bmatrix}$
Shape	95.7	$\begin{bmatrix}-0.1\\-2.4\end{bmatrix}$	$\begin{bmatrix}74\\64\\518\end{bmatrix}$
Torque	107.2	$\begin{bmatrix}-0.8\\-3.2\end{bmatrix}$	$\begin{bmatrix}114\\75\\499\end{bmatrix}$

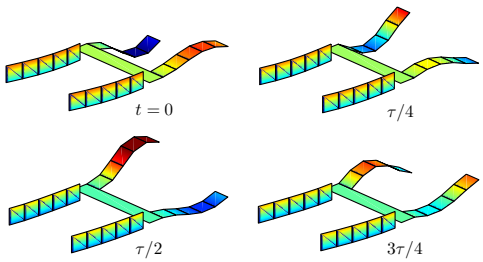

Fig. 3: Snapshots of the power optimal gait

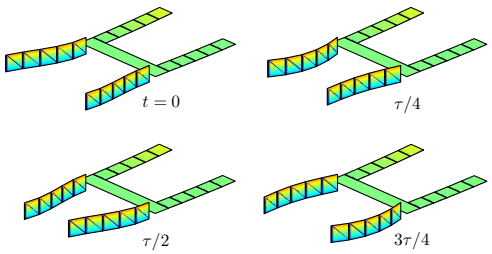

Fig. 4: Snapshots of the shape-rate optimal gait

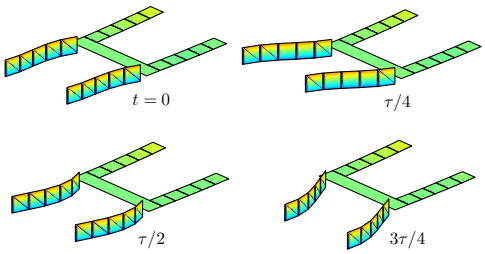

Fig. 5: Snapshots of the torque-rate optimal gait

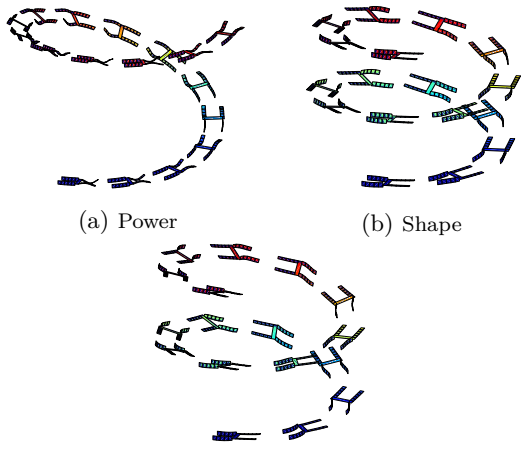

(a) Power (b) Shape (c) Torque

Fig. 6: Nonlinear model trajectory over 25 seconds

body deformation and small angular velocity harmonics. In torque-rate optimization, in particular, the pitch rate is much larger than desired. This occurs because the gait in torque-rate optimality has large roll rate harmonics due to the motion of the back panels pushing the main body from side to side, thereby violating the assumption that $\hat{\varpi}$ is of order ϵ. The roll rate harmonics can be reduced by actuating the rectifier at a higher oscillation frequency with smaller amplitudes, thereby achieving simulated velocities

that are closer to the desired values.

Figure 6 shows snapshots of the trajectories for the original nonlinear model (4) over 25 seconds.[3] The slower nominal speed and smaller yaw rate in power optimization results in a trajectory with a larger radius of rotation and a larger bank angle. The larger yaw rate and smaller roll rate in shape-derivative optimization results in a smaller radius of rotation and a tighter distance between the turns. The larger locomotion speed and pitch rate in torque-rate optimization results in the locomotor traveling at a faster pace with a larger bank angle. Despite the discrepancies between the simulated velocities, all the trajectories follow the desired path at least qualitatively, demonstrating the utility of the optimal turning gait formulation and solution for robotic locomotor designs. Although optimality of the simplified model does not guarantee global optimality for the original nonlinear model, the optimal gait found can be used as an initial condition to find optimal gaits for the fully nonlinear model.

V. Discussion and Conclusion

Analytical studies of (animal or robotic) locomotion systems require dynamic models of the body-environment interactions. While most of the past modeling efforts have addressed specific locomotor configurations, it is desired to have a "paradigm model" for a class of locomotors, upon which a general theory of locomotion can be developed. A successful paradigm model, based on geometric mechanisms, exists [6], [7], [28], [29], which encompasses modeling/analysis of locomotors interacting with environment through kinematic (nonholonomic) constraints (rolling wheels, momentum preservation, etc.). This paradigm does not capture locomotors interacting with the environment through resistive forces resulting from relative body motion (swimming, slithering) under nontrivial inertia effects. The dynamical models we developed in Section II capture this class of locomotors, providing a basis for further analytical studies.

In general, robotic locomotors are subject to many uncertainties embedded in various features, and their accurate modeling is infeasible. Hence, a good practice in robotic control design or motion planning, in our opinion, is to analyze a simple model capturing the essential dynamics and develop a rough plan for operation, followed by fine tuning on site through experiments. With this scenario in mind, we have derived the equations of motion (4) for a general class of mechanical rectifiers traveling in three dimensional space with full rotation and translation. The resistive nature of the body-environment interactions is qualitatively captured by forces linearly dependent on the relative velocities, with drag coefficients quantitatively dictating the net effect over a cycle of body oscillation. We then reduced the model to the simplest form (6) that maintained the necessary rectifying dynamics, assuming small body deformation. The state space model (6) unveils the dynamical structure of mechanical rectifiers, explicitly showing how variables are interlaced to produce thrust for propulsion and moment for turning. Our simple analytical model is not only applicable for numerical simulations, but also for theoretical study.

We then formulated an optimal turning gait problem as the minimization of a quadratic cost function subject to constraints on the average locomotion velocity and angular velocity. Physical properties (Assumption 1) were exploited to reduce the optimality problem equivalently to two separate minimization problems, solvable for globally optimal solutions. It was proven that the optimal offset resulting in turning is first found independently of the periodic term resulting in translation, while the optimal periodic term is adjusted to compensate for the environmental drag due to the shape offset. Furthermore, it was shown that, like optimal locomotion in a fixed direction, the optimal periodic term is purely sinusoidal.

To confirm the utility of the optimal gait problem and solution, numerical examples of a swimming locomotor were presented. The examples showed that while the optimality problem is formulated and solved for a simplified model, the optimal gaits are reasonable for the original nonlinear model even when the assumptions of small body deformation are slightly violated. The results showed the benefits of the optimal gait theory in finding optimal gaits that can achieve a desired trajectory and speed.

Lastly, the theoretical framework developed through a series of research, including [14] and the present paper, are useful for understanding biological mechanisms underlying animal locomotion. For instance, modeling and gait analyses within our framework have supported the hypotheses that carangiform fish exploit body-fluid resonance for efficient swimming [30] and two representative gaits of batoids, undulation and oscillation [31], result from energy optimization under round and triangular shapes of large pectoral fins [32], [33]. In the field of engineering, our framework is useful for proof-of-concept designs of mechanical rectifiers. Our theory can quickly provide a list of reasonable gaits for a creative (not necessarily bio-inspired) design of a robotic locomotor, without any *a priori* knowledge or prejudice from animal locomotion. These innovative designs of locomotors can be achieved through design/analysis iterations to go beyond mimicking what we observe in nature.

Appendix

Definitions of coefficient matrices in (4)

This section provides some details on the rectifier model in (4). Let κ be the number of rigid bodies forming the rectifier. For the i^{th} body, $m_i \in \mathbb{R}$ is the mass, $J_i \in \mathbb{R}^{3\times3}$ is the moment of inertia, $b_i(\phi) \in \mathbb{R}^3$ is the position of the center of mass relative to the center of mass of the entire system, expressed in the reference body frame, and $\psi_i^*(\phi) \in \mathbb{R}^3$ is the orientation with respect to the reference body frame. Note that b_i and ψ_i^* are functions of shape variable ϕ. The equations of motion in the body frame are

[3] A video of the simulations can be found in [27].

given by (4) for the following definitions:

$$\mathcal{J}(\phi)=\sum_{i=1}^{\kappa}\left(m_i\mathcal{Q}_i(\phi)\mathcal{Q}_i(\phi)^\intercal+\mathcal{P}_i(\phi)J_i\mathcal{P}_i(\phi)^\intercal\right),$$
$$\mathcal{C}(\phi)=\sum_{i=1}^{\kappa}\Omega(\psi_i^*)^\intercal C_i\Omega(\psi_i^*),\quad C_i:=\int\Delta_i da_i,$$
$$\mathcal{E}(\phi)=\sum_{i=1}^{\kappa}\mathcal{Q}_i(\phi)C_i\Omega(\psi_i^*),\quad D_i:=\int Q(\mathsf{c})\Delta_i Q(\mathsf{c})^\intercal da_i,$$
$$\mathcal{D}(\phi)=\sum_{i=1}^{\kappa}\left(\mathcal{Q}_i(\phi)C_i\mathcal{Q}_i(\phi)^\intercal+\mathcal{P}_i(\phi)D_i\mathcal{P}_i(\phi)^\intercal\right),$$
$$g(\phi,\dot\xi)=-\mathcal{J}(\phi)\dot\Gamma(\psi,\dot\psi)\dot\theta+\Gamma(\psi)^{-\intercal}\mathsf{G}(\theta,\dot\theta)\dot\theta,$$

where $Q(z)\in\mathbb{R}^{3\times3}$ is the skew symmetric matrix satisfying $z\times x=Q(z)x=Q(x)^\intercal z$, and

$$\mathsf{G}(\theta,\dot\theta)=\left(\frac{\partial \mathsf{J}(\theta)\dot\theta}{\partial\theta}\right)^\intercal-\frac{1}{2}\left(\frac{\partial \mathsf{J}(\theta)\dot\theta}{\partial\theta}\right),\quad \mathsf{k}(\phi):=\frac{\partial V(\phi)}{\partial\theta},$$
$$\mathsf{J}(\theta):=\Gamma(\psi)^\intercal\mathcal{J}(\phi)\Gamma(\psi),\quad \theta:=\mathrm{col}(\psi,\phi),$$
$$\mathcal{Q}_i(\phi):=\begin{bmatrix}Q(b_i)\\ \partial b_i/\partial\phi\end{bmatrix}\Omega(\psi_i^*)^\intercal,\quad \mathcal{P}_i(\phi):=\begin{bmatrix}\Omega(\psi_i^*)^\intercal\\ (\partial\psi_i^*/\partial\phi)P(\psi_i^*)^\intercal\end{bmatrix},$$
$$\Gamma(\psi):=\mathrm{diag}(P(\psi),I),\quad \dot\Gamma(\psi,\dot\psi):=\frac{d\Gamma(\psi)}{dt}.$$

It remains to show that the right hand side of the $g(\phi,\dot\xi)$ equation can be expressed in terms of ϕ, $\dot\phi$, and ϖ, without involving ψ. This is formally stated and proven in the following lemma.

Lemma 5: The function

$$\mathrm{g}(\theta,\dot\theta):=-\mathcal{J}(\phi)\dot\Gamma(\psi,\dot\psi)\dot\theta+\Gamma(\psi)^{-\intercal}\mathsf{G}(\theta,\dot\theta)\dot\theta$$

can be written as $\mathrm{g}(\theta,\dot\theta)=g(\phi,\dot\xi)$ *for some function* $g(\cdot,\cdot)$.

Proof: First note that the following identities hold for an arbitrary vector $a\in\mathbb{R}^3$:

$$\left(\frac{\partial\Omega(\psi)^\intercal a}{\partial\psi}\right)^\intercal=\Omega(\psi)^\intercal Q(a)^\intercal P(\psi),$$
$$\left(\frac{\partial P(\psi)a}{\partial\psi}\right)^\intercal\dot\psi=\dot P(\psi,\dot\psi)a,\quad \dot P(\psi,\dot\psi):=\frac{dP(\psi)}{dt},$$
$$\left(\frac{\partial P(\psi)^\intercal a}{\partial\psi}\right)\dot\psi=\mathrm{Z}(\psi,\dot\psi)a,\quad \mathrm{Z}(\psi,\dot\psi):=\frac{\partial P(\psi)\dot\psi}{\partial\psi}.$$

The function $\mathrm{g}(\theta,\dot\theta)$ can then be written as

$$\mathrm{g}(\theta,\dot\theta)=-\mathcal{J}(\phi)\begin{bmatrix}\dot P(\psi,\dot\psi)\dot\psi\\ 0\end{bmatrix}+\Gamma(\psi)^{-\intercal}\left(\left(\frac{\partial \mathsf{J}(\theta)\dot\theta}{\partial\theta}\right)^\intercal-\frac{1}{2}\left(\frac{\partial \mathsf{J}(\theta)\dot\theta}{\partial\theta}\right)\right)\dot\theta.$$

The above partial derivative terms can be simplified by:

$$\left(\frac{\partial \mathsf{J}(\theta)\dot\theta}{\partial\theta}\right)^\intercal\dot\theta=\Gamma(\psi)^\intercal\left(\frac{\partial\mathcal{J}(\phi)\dot\xi}{\partial\phi}\right)^\intercal\dot\phi+\dot\Gamma(\psi,\dot\psi)^\intercal\mathcal{J}(\phi)\dot\xi+\Gamma(\psi)^\intercal\mathcal{J}(\phi)\begin{bmatrix}\mathrm{Z}(\psi,\dot\psi)^\intercal\dot\psi\\ 0\end{bmatrix},$$
$$\left(\frac{\partial \mathsf{J}(\theta)\dot\theta}{\partial\theta}\right)\dot\theta=\begin{bmatrix}2\begin{bmatrix}\mathrm{Z}(\psi,\dot\psi) & 0\end{bmatrix}\mathcal{J}(\phi)\dot\xi\\ \dfrac{\partial\mathcal{J}(\phi)\dot\xi}{\partial\phi}\dot\xi\end{bmatrix}.$$

Using these simplifications, $\mathrm{g}(\theta,\dot\theta)$ becomes

$$\mathrm{g}(\theta,\dot\theta)=\left(\frac{\partial\mathcal{J}(\phi)\dot\xi}{\partial\phi}\right)^\intercal\dot\phi+\begin{bmatrix}\begin{bmatrix}\mathrm{R}(\psi,\dot\psi) & 0\end{bmatrix}\mathcal{J}(\phi)\dot\xi\\ -\dfrac{\partial\mathcal{J}(\phi)\dot\xi}{2\partial\phi}\dot\xi\end{bmatrix},$$

where $\mathrm{R}(\psi,\dot\psi):=P(\psi)^{-\intercal}\left(\dot P(\psi,\dot\psi)^\intercal-\mathrm{Z}(\psi,\dot\psi)\right)$. Finally, it can be shown that $\mathrm{R}(\psi,\dot\psi)=Q(\varpi)$ using the commutative property and the Jacobi identity:

$$\frac{\partial}{\partial\psi}\left(\frac{d\Omega(\psi)^\intercal a}{dt}\right)=\frac{d}{dt}\left(\frac{\partial\Omega(\psi)^\intercal a}{\partial\psi}\right),$$
$$Q(a)Q(\varpi)^\intercal+Q(\varpi)Q(a)=Q(Q(a)^\intercal\varpi).$$

Thus, $\mathrm{R}(\psi,\dot\psi)$ is a function of ϖ, and hence $\mathrm{g}(\theta,\dot\theta)$ is a function of ϕ and $\dot\xi$. ■

Some details of approximations leading to (6)

Approximate equations of motion in (6) are derived from (4), assuming that body deformation φ, angular acceleration $\dot\varpi$, and velocity components δ normal to the direction of locomotion $\mathbb{V}$ are small and of order ϵ, where $\varphi:=\phi-\eta$, $\delta:=\mathrm{N}^\intercal\nu$, $\mathrm{N}:=[\,e_1\ e_3\,]$, and e_i is the i^{th} column of the 3×3 identity matrix.

The terms in (4) can be approximated by Taylor series expansion and truncation as follows:

$$\mathcal{J}(\phi)\ddot\xi=\mathcal{J}(\eta)\ddot\zeta+\mathcal{O}(\epsilon^2),$$
$$g(\phi,\dot\xi)=\mathrm{G}(\varpi)\dot\zeta+\mathrm{G}_1(\varpi\varpi^\intercal)\varphi+\mathcal{O}(\epsilon^2),$$
$$\mathcal{D}(\phi)\dot\xi=\mathcal{D}(\eta)\dot\zeta+\mathrm{D}_1(\varpi)\varphi+\mathcal{O}(\epsilon^2),$$
$$\mathcal{E}(\phi)\nu=\cancel{\mathcal{E}(\eta)e_2v}+\mathcal{E}(\eta)\mathrm{N}\delta+v\Lambda\varphi+\mathcal{O}(\epsilon^2),$$
$$\mathsf{k}(\phi)=\cancel{\mathsf{k}(\eta)}+\mathrm{K}\varphi+\mathcal{O}(\epsilon^2),$$
$$\mathrm{N}^\intercal Q(\varpi)\nu=v\mathcal{R}\varpi+\mathrm{N}^\intercal Q(\varpi)\mathrm{N}\delta,$$
$$e_2^\intercal Q(\varpi)\nu=-(\mathcal{R}\varpi)^\intercal\delta,$$
$$\mathrm{N}^\intercal\mathcal{C}(\phi)\nu=\cancel{\mathrm{N}^\intercal\mathcal{C}(\eta)e_2v}+\mathrm{N}^\intercal\mathcal{C}(\eta)\mathrm{N}\delta+v\mathcal{Q}\varphi+\mathcal{O}(\epsilon^2),$$
$$e_2^\intercal\mathcal{C}(\phi)\nu=\cancel{e_2^\intercal\mathcal{C}(\eta)\mathrm{N}\delta}+c(\varphi)v+(\mathcal{Q}\varphi)^\intercal\delta+\mathcal{O}(\epsilon^3),$$
$$\mathrm{N}^\intercal\mathcal{E}(\phi)^\intercal\dot\xi=\mathrm{N}^\intercal\mathcal{E}(\eta)^\intercal\dot\zeta+\mathrm{E}(\varpi)\varphi+\mathcal{O}(\epsilon^2),$$
$$e_2^\intercal\mathcal{E}(\phi)^\intercal\dot\xi=\cancel{e_2^\intercal\mathcal{E}(\eta)^\intercal\dot\zeta}+(\Lambda\varphi)^\intercal\dot\zeta+\varphi^\intercal\mathrm{F}(\varpi)\varphi+\mathcal{O}(\epsilon^3),$$

where $\dot\zeta:=\mathrm{col}(\varpi,\dot\varphi)$ and $v:=e_2^\intercal\nu$. Functions G, G_1, D_1, E, and F are linear (without constant terms) and function $c(\varphi)$ is the quadratic approximation of $e_2^\intercal\mathcal{C}(\phi)e_2$. All the terms depend on η and the canceled terms are zero due to the nominal shape properties. Thus, (4) approximates to

$$J\ddot\zeta+D(\varpi)\dot\zeta+K(\varpi,v)\varphi+E\delta=Bu,$$
$$m\dot\delta+C(\varpi)\delta+m\mathcal{R}\varpi v+E^\intercal\dot\zeta+\mathrm{L}(\varpi,v)\varphi=0,$$
$$m\dot v+c(\varphi)v+(\mathcal{Q}\varphi-m\mathcal{R}\varpi)^\intercal\delta+(\Lambda\varphi)^\intercal\dot\zeta+\varphi^\intercal\mathrm{F}(\varpi)\varphi=0,$$

where $\mathcal{O}(\epsilon^2)$ and $\mathcal{O}(\epsilon^3)$ terms are neglected in the first two and the last equations, respectively, and

$$J:=\mathcal{J}(\eta),\quad E:=\mathcal{E}(\eta)\mathrm{N},\quad D(\varpi):=\mathcal{D}(\eta)+\mathrm{G}(\varpi),$$
$$\mathrm{L}(\varpi,v):=v\mathcal{Q}+\mathrm{E}(\varpi),\quad C(\varpi):=\mathrm{N}^\intercal(mQ(\varpi)+\mathcal{C}(\eta))\mathrm{N},$$
$$K(\varpi,v):=\mathrm{G}_1(\varpi\varpi^\intercal)+\mathrm{D}_1(\varpi)+v\Lambda+\mathrm{K},$$

Finally, it can readily be seen that the approximate equations can be expressed in a more compact form as (6).

References

[1] R. W. Brockett, "On the rectification of vibratory motion," *Sensors Actuators*, vol. 20, pp. 91–96, 1989.

[2] M. H. Dickinson, C. T. Farley, R. J. Full, M. A. R. Koehl, R. Kram, and S. Lehman, "How animals move: an integrative view," *Science*, vol. 288, no. 5463, pp. 100–106, 2000.

[3] R. D. Beer, "A dynamical systems perspective on agent-environment interaction," *Artificial intelligence*, vol. 72, no. 1–2, pp. 173–215, 1995.

[4] G. Bessonnet, S. Chesse, and P. Sardain, "Optimal gait synthesis of a seven-link planar biped," *Int. J. of Robot. Res.*, vol. 23, no. 10–11, pp. 1059–1073, 2004.

[5] G. Hicks and K. Ito, "A method for determination of optimal gaits with application to a snake-like serial-link structure," *IEEE Trans. Autom. Control*, vol. 50, no. 9, pp. 1291–1306, 2005.

[6] J. Cortés, S. Martínez, J. P. Ostrowski, and K. A. McIsaac, "Optimal gaits for dynamic robotic locomotion," *Int. J. of Robot. Res.*, vol. 20, no. 9, pp. 707–728, 2001.

[7] J. P. Ostrowski, J. P. Desai, and V. Kumar, "Optimal gait selection for nonholonomic locomotion systems," *Int. J. of Robot. Res.*, vol. 19, no. 3, pp. 225–237, 2000.

[8] T. Saidouni and G. Bessonnet, "Generating globally optimised sagittal gait cycles of a biped robot," *Robotica*, vol. 21, no. 2, pp. 199–210, 2003.

[9] M. Srinivasan and A. Ruina, "Computer optimization of a minimal biped model discovers walking and running," *Nature*, vol. 439, no. 7072, pp. 72–75, 2006.

[10] K. Nagasaka, H. Inoue, and M. Inaba, "Dynamic walking pattern generation for a humanoid robot based on optimal gradient method," in *IEEE Int. Conf. Syst., Man, and Cybern.*, vol. 6, 1999, pp. 908–913.

[11] C. Chevallereau and Y. Aoustin, "Optimal reference trajectories for walking and running of a biped robot," *Robotica*, vol. 19, no. 5, pp. 557–569, 2001.

[12] M. Saito, M. Fukaya, and T. Iwasaki, "Modeling, analysis, and synthesis of serpentine locomotion with a multilink robotic snake," *IEEE Control Syst. Mag.*, vol. 22, no. 1, pp. 64–81, 2002.

[13] K. A. McIsaac and J. P. Ostrowski, "Motion planning for anguilliform locomotion," *IEEE Trans. Robot. Auto.*, vol. 19, no. 4, pp. 637–652, 2003.

[14] J. Blair and T. Iwasaki, "Optimal gaits for mechanical rectifier systems," *IEEE Trans. Autom. Control*, vol. 56, no. 1, pp. 59–71, 2011.

[15] D. J. Cho, J. H. Kim, and D. G. Gweon, "Optimal turning gait of a quadruped walking robot," *Robotica*, vol. 13, no. 6, pp. 559–564, 1995.

[16] D. K. Pratihar, K. Deb, and A. Ghosh, "Optimal turning gait of a six-legged robot using a GA-fuzzy approach," *Artificial Intell. for Eng. Design, Anal. and Manuf.*, vol. 14, no. 3, pp. 207–219, 2000.

[17] Z. Bien, M. G. Chun, and H. S. Son, "An optimal turning gait for a quadruped walking robot," in *IEEE/RSJ Int. Workshop on Intelligent Robots and Syst.*, 1991, pp. 1511–1514.

[18] S. Miao and D. Howard, "Optimal tripod turning gait generation for hexapod walking machines," *Robotica*, vol. 18, no. 6, pp. 639–649, 2000.

[19] C. Ye, S. Ma, B. Li, and Y. Wang, "Turning and side motion of snake-like robot," in *IEEE Int. Conf. on Robot. and Auto.*, vol. 5, 2004, pp. 5075–5080.

[20] S. Kohannim and T. Iwasaki, "Optimal turning gait for mechanical rectifier systems with three dimensional motion," in *IEEE Conf. Decision Control*, 2014, pp. 5862–5867.

[21] ——, "Optimal turning gait for undulatory locomotion," in *Proc. Amer. Control Conf.*, 2012, pp. 3459–3464.

[22] G. Taylor, "Analysis of the swimming of long and narrow animals," in *Proc. R. Soc. of London A*, vol. 214, no. 1117, 1952, pp. 158–183.

[23] J. Chen, W. O. Friesen, and T. Iwasaki, "Mechanisms underlying rhythmic locomotion: body–fluid interaction in undulatory swimming," *J. of Exp. Biol.*, vol. 214, no. 4, pp. 561–574, 2011.

[24] H. K. Khalil, *Nonlinear systems*. New Jersey: Prentice hall, 1996, vol. 3.

[25] A. L. Fradkov and V. A. Yakubovich, "The S-procedure and duality relations in nonconvex problems of quadratic programming," *Vestn. LGU, Ser. Mat., Mekh., Astron*, vol. 6, pp. 101–109, 1979.

[26] R. E. Skelton, T. Iwasaki, and D. E. Grigoriadis, *A unified algebraic approach to control design*. CRC Press, 1997.

[27] CyCLab. (2016) Optimal gaits for locomotion systems. [Online]. Available: http://www.seas.ucla.edu/~iwasaki/lab.html

[28] G. S. Chirikjian and J. W. Burdick, "The kinematics of hyper-redundant robot locomotion," *IEEE Trans. Robot. Auto.*, vol. 11, no. 6, pp. 781–793, 1995.

[29] F. Boyer and M. Porez, "Multibody system dynamics for bio-inspired locomotion: from geometric structures to computational aspects," *Bioinspiration & biomimetics*, vol. 10, no. 2, 2015.

[30] S. Kohannim and T. Iwasaki, "Analytical insights into optimality and resonance in fish swimming," *J. R. Soc. Interface*, vol. 11, no. 92, 2014.

[31] L. J. Rosenberger, "Pectoral fin locomotion in batoid fishes: undulation versus oscillation," *J. Exp. Biol.*, vol. 204, no. 2, pp. 379–394, 2001.

[32] X. Liu, T. Iwasaki, and F. Fish, "Dynamic modeling and gait analysis of batoid swimming," in *Proc. Amer. Control Conf.*, 2013, pp. 566–571.

[33] X. Liu, F. Fish, R. S. Rusho, S. S. Blemker, and T. Iwasaki, "Modeling and optimality analysis of pectoral fin locomotion," in *Neuromechanical Modeling of Posture and Locomotion*. Springer, 2016, ch. 11, pp. 309–332.

Saba Kohannim received her B.S. and M.S. degrees in Mechanical Engineering from University of California, Los Angeles in 2011 and 2013, respectively, and is currently pursing the Ph.D. degree in Mechanical Engineering (with a concentration in systems and control) at the Department of Mechanical and Aerospace Engineering (MAE) at UCLA. She was awarded the NSF Graduate Research Fellowship in 2013.

Her research interests include optimal control for biological locomotion, nonlinear and chaotic oscillators, multi-agent coordination, and neuronal networks.

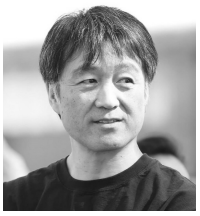

Tetsuya Iwasaki (M'90-SM'01-F'09) received his B.S. and M.S. degrees in Electrical and Electronic Engineering from the Tokyo Institute of Technology (Tokyo Tech) in 1987 and 1990, respectively, and his Ph.D. degree in Aeronautics and Astronautics from Purdue University in 1993. He held a Post-Doctoral Research Associate position at Purdue University (1994-1995), and faculty positions at Tokyo Tech (1995-2000) and at the University of Virginia (2000-2009), before joining the UCLA faculty as Professor of Mechanical and Aerospace Engineering.

Dr. Iwasaki's current research interests include biological control mechanisms underlying animal locomotion, nonlinear oscillators, and robust/optimal control theories and their applications to engineering systems. He has received CAREER Award from NSF, Pioneer Prize from the Society of Instrument and Control Engineers, George S. Axelby Outstanding Paper Award from IEEE, Rudolf Kalman Best Paper Award from ASME, and Steve Hsia Biomedical Paper Award at the 8th World Congress on Intelligent Control and Automation. He has served as associate editor of *IEEE Transactions on Automatic Control*, *Systems & Control Letters*, *IFAC Automatica*, *International Journal of Robust and Nonlinear Control*, and *SIAM Journal on Control and Optimization*.